The Timing of Sensory-Guided Behavioral Response is Represented in the Mouse Primary Somatosensory Cortex

Jeremy Camon, Sandrine Hugues, Melissa A Erlandson, David Robbe, Sabria Lagoun, Emna Marouane, Ingrid Bureau

The timing of sensory-guided behavioral response is represented in the mouse primary somatosensory cortex

Jérémy Camon*[1], Sandrine Hugues*[1], Melissa A. Erlandson[1], David Robbe[1], Sabria Lagoun[1], Emna Marouane[1] and Ingrid Bureau[1]

* contributed equally

1, INMED, INSERM U1249, Université Aix-Marseille, Marseille, France.

Corresponding author:

Ingrid Bureau

INMED, INSERM U1249

163 route de Luminy, 13009 Marseille (France)

Tel : +33 491 828 127

Fax: +33 491 828 101

Email: ingrid.bureau@inserm.fr

Running title: The S1 representation of the timing of behavioral responses

Abstract

Whisker-guided decision making in mice is thought to critically depend on information processing occurring in the primary somatosensory cortex. However, it is not clear if neuronal activity in this "early" sensory region contains information about the timing and speed of motor response. To address this question we designed a new task in which freely moving mice learned to associate a whisker stimulus to reward delivery. The task was tailored in such a way that a wide range of delays between whisker stimulation and reward collection were observed due to differences of motivation and perception. After training, mice were anesthetized and neuronal responses evoked by stimulating trained and untrained whiskers were recorded across several cortical columns of barrel cortex. We found a strong correlation between the delay of the mouse behavioral response and the timing of multi-unit activity evoked by the trained whisker, outside its principal cortical column, in layer 4 and 5A but not in layer 2/3. Circuit mapping *ex vivo* revealed this effect was associated with a weakening of layer 4 to layer 2/3 projection. We conclude that the processes controlling the propagation of key sensory inputs to naive cortical columns and the timing of sensory-guided action are linked.

Keywords: barrel, circuit, learning, perceptual decision, plasticity

Introduction

Animals must process a wide array of sensory information to select adaptive actions. For instance, depending on the presence or absence of a visual stimulus that signals the proximity of a predator (e.g., a bird-looking moving shadow), a mouse will decide either to run back toward its burrow or continue its outdoor foraging for food. Recently, it has been proposed that this type of perceptual decision might rely on parallel neural processes operating across a wide range of brain regions (Cisek and Kalaska 2010). For example, multiple actions which could be performed are represented in a pre-motor region during presentation of sensory cues, before the actual choice has been made (Cisek and Kalaska 2005). Conversely when rodents learn to perform a conditioned motor response when they detect a stimulation of their whiskers (e.g., licking from a reward spout), neuronal activity in the barrel cortex is predictive of the occurrence or lack of behavioral response (Sachidhanandam et al. 2013; Yang et al. 2016). Interestingly, in this early sensory cortical region, behavioral decisions do not only correlate with firing rate but also with the precise timing of whisker-evoked spikes (Zuo et al. 2015). Altogether, these studies suggest that activity in primary sensory cortical areas determines what actions will be selected later on. In order to behave in an adaptive manner, animals must not only choose the most appropriate action according to available sensory information, but react and perform actions with appropriate timing and speed. In a laboratory setting, the design of a task may require animals to wait for a delayed go signal to report their choice. Animals modulate also the speed and accuracy of their response to adapt to the payoff and the cost of errors (Reinagel 2013; Bermudez and Schultz 2014). So far, the delay of behavioral responses has been found to be represented in associative and motor regions through accumulative activities that eventually pass a threshold (Gold and Shadlen 2007).

It is not known whether changes in neuronal activity in primary sensory cortices are associated to changes in behavioral timing.

To address this question, we developed a new task in which mice must learn to run to collect a reward following the stimulation of whiskers (hereafter called trained whiskers). After training and behavioral testing, we recorded during anesthesia the responses of neuronal populations across the layers of the barrel cortex to the deflection of either the trained or adjacent non-trained whiskers. Recording were performed in the cortical column corresponding to the trained whiskers and in adjacent columns. We report that the delay of multi-unit activity (MUA) responses to the trained whisker stimulation evoked in the adjacent cortical column was highly correlated to the behavioral delay expressed by the animal in response to the whisker stimulation in the task. Our data provide novel insight on how activity in an early sensory cortical area can be predictive of how animals respond to sensory cues.

Materials and Methods

All experimental procedures were conducted in accordance with standard ethical guidelines (European Communities Directive 86/60-EEC) and were approved by an ethical committee (Ministère de l'enseignement supérieur et de la recherche, France, Ref 00094.01).

Behavior. After one week of handling and habituation to the arena, 8 week old C57Bl6 male mice (n = 52) were lightly anesthetized (ketamin, 65 $mg.kg^{-1}$; xylazin, 5 $mg.kg^{-1}$) and equipped with metal rods (1.5 mm) glued on the C1 and C2 whiskers at 7 mm from the skin and with an Elizabethan collar (Gdalyahu et al. 2012). Whiskers were shortened to ~ 1.5 cm. After two days of recovery, they were conditioned in the bore (18 cm diameter) of an electrical magnet to poke

their snout in a water port in order to get a drop of water (50 µl). Mice were water restricted to ~ 1 ml per day during the training sessions and were given more water after to adjust their weight loss to < -15 % (-10 ± 1 % at the sixth session). They had food *ad libitum*. The animals received five sessions in five days, then two to three days of rest during which they had free access to water until 24 hours before a final sixth session of training. A session was a succession of go and catch trials in pseudo random order. They were of 21 s each interleaved by a minimum of 20 s if no water was delivered or 40 s after a rewarded go trial. A go trial was initiated when a mouse reached the edge of the arena diametrically opposite of the water port (Fig. 1B), but the exact time was not otherwise explicitly cued. Then, whisker stimulus was delivered immediately through the oscillation of the magnetic field (13 mT) at 8 Hz, irrespectively of whether the animal was whisking or not. Its duration varied between three and ten seconds and ceased at the same time the reward was delivered. The oscillations deflected the whiskers by 1.5 mm when the animal was on its four paws and 1 mm when it was rearing (tested on anesthetized mice; amplitudes measured at the level of the metal rod). When deflected, the C whiskers did not touch the other whiskers. The water port was inactivated during the first three seconds of whisker stimulations after which it became operational until the tenth second of trial. A camera above the arena detected the presence of the black mouse at the water port thanks to contrast with the white platform (Fig. 1B). Catch trials started similarly to go trials but were without whisker stimulation and the water port was inactivated at all times. A session was interrupted when a mouse stopped going to the water port on three consecutive go trials. The number of go trials was 12 - 22 (average, 17.5) at the last session. Total stimulation time was 32 to 114 s (average, 72 s). About 50 % of animals lost one metal rod over the course of training and only C1 or C2 was stimulated for the remaining sessions. Animals tested without a whisker cue (Fig. 1D) were three mice that had lost the two metal rods between the fifth and last session. Animals tested for whisker

selectivity (Fig. 1E) were anesthetized after five or six sessions to reposition the metal rods on the B1 and B2 whiskers and were tested again the day after. The bottle was returned to the animal after the last training session until electrophysiology was performed the day after.

Analysis of behavior. The delay prior the first visit of the water port since the initiation of a trial (or nose poke delay, NPD) was measured in go and catch trials. For go trials, NPD is also the delay since the onset of whisker stimulation. The length of visits (Fig. 1F) is the time spent in front the water port during the delay period. Its maximum value is 3 s. A defensive behavior is characterized by rearing accompanied of head-shaking movements, backing up or pivoting. 65 % of mice exhibited whisker-triggered defensive behavior (Fig. 1H,I), meaning they displayed this behavior more frequently during whisker stimulation than in catch trials. We found mice that had kept two metal rods until the end of training were more prone to having defensive behavior: the rate was 82 % and 52 % of mice that had two and one metal rod, respectively. Having one or two metal rods did not impact NPD per se in a significant way. In the group with defensive behavior, NPD was 5.1 ± 1.8 s and 4.1 ± 2.2 s for mice with two or one metal rod respectively (mean ± SD; n = 25 and 22; $p = 0.16$, Mann-Whitney test). In the group without defensive behavior, NPD was 3.7 ± 0.7 s and 3.6 ± 1.4 s for mice with two or one metal rod respectively (n = 4 and 12; $p = 0.81$). Thus, variability was large in every group suggesting the number of stimulated whiskers, 1 or 2, was not a main factor modulating NPD.

***In vivo* electrophysiology.** Mice were anesthetized with 130 $mg.kg^{-1}$ ketamin and 10 $mg.kg^{-1}$ xylazin and placed in a stereotaxic apparatus. Lidocaine was administered at the site of skin incision. Depth of anesthesia was monitored by hindpaw reflexes and spontaneous movements of whiskers. One supplemental injection of the anesthetic mix at 50 % of the initial dose was

administered about two hours later. Body temperature was maintained at 39°C with a feedback temperature controller (CWE Inc., Ardmore, Pennsylvania). Ophtalmic gel was placed on both eyes to prevent drying. A craniotomy (4 × 4 mm) was made to expose the barrel field. The brain was hydrated with saline solution (0.09 % NaCl). The dura was removed and a 8 × 4 32 channels silicon probe (15 μm thick shanks, 413 μm^2 sites, 200 μm spacing; Neuronexus, Ann Arbor, Michigan) oriented at 45° from the middle line was lowered orthogonally to the brain over the arc 1 or arc 2 of the barrel field until the middle of the top electrodes was at the surface of the brain. The most lateral shank was at + 4.1 mm lateral and -2 mm posterior from bregma. The reference electrode was at the junction of the brain and cerebellum. The whiskers A, B, C and D, arc 1 then arc 2 were placed in glass capillaries mounted onto electrical benders (PI France, Aix-en-Provence, France). The tip of capillaries was at ~ 7 mm of the skin. A first round of deflections was performed to choose between deflecting arc 1 or arc 2 for the rest of the recording. 18-36 trains of three deflections were delivered to each whisker with an interval between trains of 3 or 6 s. Each deflection measured at the tip of the capillary was ~ 750 μm accomplished in 6 or 10 ms along the caudo-rostral axis, followed 200 ms later by a move backward of same design. Intervals between deflections in a train were 200 ms. We did not aim to reproduce the whisker stimulus delivered in the behavioral arena. This would be difficult to accomplish because the amplitude and direction of whisker deflections varied on a moment-to-moment basis during the train of electromagnetic pulses, depending on the mouse position and its head posture in the arena. In addition, whisker-evoked cortical activation most likely varied according to the behavioral state of the animal during the stimulation. Signals were digitized at 10 kHz with an Xcellamp amplifier (Dipsi, Cancale, France).

***In vivo* data analysis.** All analysis was performed offline with routines written in Matlab (MathWorks, Natick, Massachusetts). Traces were filtered with a Butterworth 500-3000 Hz bandpass filter. The threshold for detecting spikes was set independently for each channel as 3.5 × root mean square (rms) of the signal in baseline. The minimum amplitude of a spike decaying slope was set to rms and its maximum duration to 0.2 ms. Spikes were then binned every 1 ms. The MUA evoked by the whisker stimulus at each recording site is averaged across trials and the mean baseline activity averaged in the 400 ms period preceding each train of deflection was subtracted. For each mouse, three to four shanks of electrodes where the deflection of the whiskers A, B, C and D evoked the largest responses were used for further analysis. In general, two shanks selected this way with a clear functional principal whisker each were separated by one shank where the two whiskers evoked responses of similar amplitudes. In Fig. 3-4, only the recording sites where responses to the principal whisker were greater than four spikes in 40 ms were included in the analysis. The mean spike delay (msd) of MUA is: Σ (spike x delay from the stimulation onset)/ Σ (spike). The latencies to 25 % of the peak amplitude were used as a proxy for the response onset and end. Cross-correlograms (CCG) were generated for MUA signal recorded in adjacent columns (B and C), same layer. CCG were corrected with a jitter-based method to remove correlations due to the firing rate fluctuations locked to the stimulus and keep short time scale correlations. Surrogate data sets (100) were generated in which each spike was replaced by another spike chosen randomly from the set of spikes evoked in the same 50 ms bin across all trials (Smith and Kohn 2008). The correction term is the average CCG computed with these surrogates and is subtracted from the raw CCG. The significance level is the correction term plus twice the standard deviation.

In vitro **electrophysiology and laser scanning photostimulation (LSPS) with glutamate uncaging.** Data from naive mice were used in a previous study describing LSPS combined with extracellular recordings (Erlandson et al. 2015). Data from naive and trained mice were acquired in the same period. Mice received an intraperitoneal injection of a Ketamine/Xylazine mix (65 $mg.kg^{-1}$, 5 $mg.kg^{-1}$) and a cervical dislocation prior to decapitation. Across-row barrel cortex slices (300 µm thick) were prepared as described (Finnerty et al. 1999) in an ice-cold solution containing (in mM): 110 choline chloride, 25 $NaHCO_3$, 25 D-glucose, 11.6 sodium ascorbate, 7 $MgCl_2$, 3.1 sodium pyruvate, 2.5 KCl, 1.25 NaH_2PO_4, and 0.5 $CaCl_2$. Slices were transferred to artificial cerebrospinal fluid (ACSF) containing (in mM): 127 NaCl, 25 $NaHCO_3$, 25 D-glucose, 2.5 KCl, 1 $MgCl_2$, 2 $CaCl_2$, and 1.25 NaH_2PO_4, aerated with 95 % O_2 and 5 % CO_2, first at 34°C for 15 minutes and then at room temperature prior to use. ACSF was complemented with (in mM): 0.2 MNI-caged glutamate (Tocris, Bristol, UK), 0.005 (±)-CPP (Sigma) an antagonist of NMDA receptors, 4 $CaCl_2$ and 4 $MgCl_2$ for LSPS mapping. Recordings were performed at room temperature in the B and C whisker columns of arc 1 (or arc 2 if the animal had lost the metal rod on C1). The slice containing arc 1 has five barrels A B C D E. It is the last slice with a ventricle or the one immediately more medial and is followed by a slice with only four barrels corresponding to the α β γ δ whiskers. Thin borosilicate electrodes with low resistance (0.5-1 MΩ) were filled with extracellular medium and lowered ~120 µm deep into the tissue. Slices illuminated with infra-red light were inspected so as to place the pipettes in the layer 2/3 above the barrels B and C. We previously showed that the properties of maps generated from layer 2 and layer 3 changed in a continuum (Erlandson et al. 2015). Hence, the divide between the two layers was set arbitrarily at mid-distance between bottom layer 1 and top layer 4. Traces were sampled at 10 kHz and filtered at 800 Hz (Multiclamp 700b, Molecular devices, Sunnyvale, California). 50/60 Hz noise and harmonics were removed with a noise eliminator (HumBug,

Quest Scientific, Cumming, Georgia). Focal photolysis of caged glutamate was accomplished with a 2 ms 20 mW pulse of a UV (355 nm) laser (DPSS Lasers Inc., Santa Clara, California) through a 0.16 NA 4 × objective (Olympus, Center Valley, Pennsylvania). The full optical pathway and scanning system are described in (Shepherd and Svoboda 2005). The stimulus pattern consists of 256 positions on a 16 × 16 grid (75 μm spacing). The uncaging grid was centered vertically between the barrels B and C. The ninth and tenth lines of the grid were above L4 and L5A, respectively (layer 5A is a light band below layer 4). The UV stimuli were presented once every 700 ms in a spatial order designed to avoid consecutive glutamate uncaging at neighboring sites (Shepherd et al. 2003). Four maps with different sequential orders of UV stimulations were acquired for every pipette position. Custom software for instrument control and acquisition (Suter et al. 2010) was written in Matlab

***In vitro* data analysis.** Analysis was performed offline with a routine written in Matlab. Traces were smoothed with a 2 ms sliding window. The four traces evoked at every uncaging site were averaged to construct mean single-position maps. A detailed study of local field potentials evoked by glutamate uncaging in a slice is in Erlandson et al. 2015. Briefly, uncaging evoked direct responses and mono-synaptic responses. Thus, there were no poly-synaptic events in our conditions. Direct responses arose during the laser pulse and were either negative or positive depending on the distance between the pipette tip and the locus of uncaging (negative events were evoked close to the tip). Synaptic events were evoked with a delay > 4 ms and synaptic input maps were computed based on the peak amplitude of negative potentials that were within 5-50 ms after the stimulus onset. Single-position maps were then used to generate a group-average map. Group-average maps from the B or C column (Fig. 5C) were realigned to show the recording sites aligned vertically. Maps from the B and C columns of naive mice were merged.

Results

Variably long delays precede the behavioral response of mice in a go/catch task

To investigate the neural mechanisms contributing to the timing of sensory-guided behavioral responses, we developed a task in which water-restricted mice, freely exploring a circular arena, learned to collect a reward from a water port following a prolonged stimulation of their whiskers. A metal rod was glued to two C whiskers and remote whisker stimulation was achieved by applying an oscillating (8 Hz) magnetic field to the arena. While the mouse could approach the water port at any time, reward was delivered only three seconds after the whisker stimulation onset (Fig. 1A-C). The timing of whisker-guided behavioral response was measured as the delay between the whisker stimulation onset and the animal nose poke in the reward port (thereafter referred to as nose poke delay, NPD; see Methods). To avoid that the distance of the animals to the water port biased NPD, whiskers stimulation were triggered when animals entered a region of the arena diametrically opposite to the reward port (stimulation area, no visible marker for the mice, Fig 1B). Behavioral sessions were composed of go trials (stimulation was turned on when animals entered the stimulation area) and catch trials (mice entered the stimulation area but stimulation was not turned on). NPD were measured from the moment animals entered the stimulation area until the moment they eventually reached the water port. The catch trials allowed testing whether animals responded specifically to the whisker stimulation or if they simply checked compulsively the water port. Mice were trained for six sessions and NPD were measured during the sixth session. On average mice made their first nose poke at the water port 5.4 ± 2.2 s after stimulation onset (mean ± SD ; n = 52 mice). The variability was large even when considering a single animal (Fig. 1B,C). Such variability is explained by the fact that NPD

increased over the course of the session, to the point that the number of trials in which mice never collected a reward increased too. This observation suggested that the animal motivation contributed to the NPD. When the first five trials were considered, a period during which mice never missed going to the water port after whisker stimulation, NPD during go trials decreased by ~ 1 s and was 4.3 ± 1.9 s (mean ± SD). NPD during catch trials were ~ 2 s longer (6.1 ± 3.0 s; p = 0.0005 paired Wilcoxon test). To test if this effect was due to the stimulation of whiskers rather than to an uncontrolled perception of the magnetic field oscillation, we examined the performance of three mice that had lost their metal rod between the 5th and 6th sessions. In these mice, NPD dramatically increased in go trials from 3.7 ± 0.3 s (mean ± SEM; first 5 trials) at the 5th session to 10.4 ± 1.0 s at the 6th and was similar to NPD of catch trials (9.9 ± 2.2 s; Fig. 1D). We also examined if mice, after having learned to associate the stimulation of their C whiskers with reward availability at the water port, generalized this associative learning to another row of whiskers. For this, we moved the metal rod from the C to the B whiskers. After the switch, NPD at the first go trial increased to almost match the NPD of the first catch trial but the gap between go and catch reappeared in subsequent trials (Fig. 1E). This pattern was different from that observed during initial learning at the first training session (Fig. 1E, in gray) showing that the change of stimulated whisker did not reset learning. Rather, the brief overlap of NPD from go and catch trials suggests that mice were perturbed by the change but this perturbation was transient and learning quickly transferred from the initial whisker row to the neighboring one. An important aspect of our task design was that reward was available only three seconds after the whisker stimulation was turned on (Fig 1A). Thus, in a fraction of trials, mice reached the water port before being actually rewarded. In some cases the mice did not wait for the end of this 3 s delay period and left. In other cases the mice stayed until the end. We compared how long, during the delay period, mice stayed at the water port in go and catch trials and found that mice stayed

longer in go trials (Fig. 1F,G; Wilcoxon test, $p = 0.02$). Thus, these results show that in go trials mice biased their behavior in two ways upon whisker stimulation. First, they ran toward the reward area with shorter delays. Second, when mice arrived too early at the water port, they stayed longer there until reward was actually delivered. Finally, we investigated whether internal factor such as motivation accounted for the variability of NPD that remained large even after restricting our analysis to the first five trials. Motivation likely triggered visits of the water port in the absence of whisker stimulus so we compared NPD measured in catch trials and go trials. These were positively correlated, even if relatively weakly (Spearman correlation coefficient, r = 0.3; $p = 0.02$; n = 52). This suggested that motivation was influential but probably not the only factor that explained the inter-individual variability of NPD. We then studied the mouse behavior while it was being stimulated before it approached the water port. 65 % of them exhibited whisker-triggered defensive behavior (He et al. 2017; see Methods). Excluding these mice reduced behavioral delays by ~ 1 s (NPD = 3.5 ± 0.3 s; n = 18) but the range was still of several seconds (1.6 – 6.3 s; Fig. 1H). The correlation between NPDs from go and catch trials increased (r = 0.5; $p = 0.04$; Fig.1I) indicating that motivation was a better predictor of behavioral timing for mice without whisker-evoked defensiveness. There was no significant correlation for others (r = 0.3; $p = 0.09$; n = 34*).* Hence, multiple factors contribute in modulating the timing of whisker-guided behavioral responses in the task, among them motivation and the perception, as being innocuous or bothersome, of the whisker stimulus.

Training changed the temporal properties of multi-unit activity evoked by secondary whiskers

The aforementioned behavioral results showed that trained animals learned to detect the stimulation of their whiskers and effectively used this sensory cue to guide their reward-directed

behavior. To examine if this form of associative learning was associated with changes in functional neural activity in the primary sensory barrel cortex, we recorded the whisker-evoked multi-unit spiking activity (MUA) in the barrel cortex, one day after the last training session. Extracellular electrophysiological recordings were performed under anesthesia with a 32 channel silicon probe (8 shanks, 4 sites per shank, distances between shanks and recording sites: 200 µm) which allowed to record MUA across layers and several columns in response to deflection of different whiskers using glass capillaries (A, B, C and D, Fig. 2A1, Methods). Responses were recorded at four depths (20, 220, 420 and 620 µm) in 3-4 cortical columns simultaneously. We selected four shanks of the probe where the whisker deflections evoked their largest responses and each shank was assigned a functional principal whisker (PW) as well as secondary and tertiary whiskers (SW, TW) on the basis of the size of responses (see Fig. 2A2 and Methods). While there was very little MUA at the most superficial recording, MUA evoked by the principal whiskers at depths 2, 3 and 4 showed properties consistent with the layer 2/3, the layer 4 and the layer 5A respectively: layer 2/3 had the lowest evoked firing rate and layer 4 the strongest; layer 2/3 and layer 5A MUA had stronger short depression during the stimulation trains; and layer 5A had delayed responses and the lowest selectivity for the principal whisker over the secondary whiskers (Fig. 2B,C1 and Table 1; Ahissar et al. 2001). Although some of these parameters changed after mice were trained, three layers could still be resolved (Fig. 2C2 and Table 1).

First, we compared recordings performed in trained mice (n = 38) and naive mice (n = 20; these were not water-restricted and never explored the test arena), to study the overall effects of the conditioning. We measured MUA in the cortical column of barrel cortex functionally connected to the stimulated whisker and in neighboring columns. Surprisingly there was little change in MUA evoked by PW, except that in trained mice, the responses returned to baseline more rapidly in all layers (see Fig 2D for the case of layer 4; table 1). However training had a pronounced

effect on the responses to SW deflections. First their peak amplitude was increased in trained mice compared to naive and this effect was present across layers and was not restricted to the trained whisker (see Fig 2D for the case of layer 4; table 1). Moreover, responses to SW, trained or non-trained, changed shape: they reached a peak after shorter delays and they returned more quickly to baseline in trained mice (Fig 2D). The re-alignment of responses around their center of mass showed clearly this effect (Fig 2E,F) and suggested it reflected a decreased variability in spike timing (Fig 2E). Furthermore, the spike density integrated over the whole response was unchanged for layer 4 and 5A and even decreased in layer 2/3 (-20 %; Fig. 2G) indicating that the increased peak amplitude of responses to SW described earlier was also due to a temporal redistribution of spikes. An increased reliability in spike timing could indicate an enhanced coherence of firing between neurons of trained mice. To test this, we cross-correlated MUA signal (Berger et al. 2007) evoked by a whisker in its primary column and the adjacent one (Fig. 2H; see Methods). Raw CCG were corrected with a jitter-based method in order to eliminate correlations due to the firing rate variations driven by stimulation. 30 % of all pairs (21/70) showed significant correlations in naive mice. This ratio was 60 % after training (37/62; Fig. 2I). Altogether this set of data reveals the plasticity of neuronal activity in trained mice under the form of faster and sharper population responses to deflection of secondary whiskers that suggests a form of temporal coding.

The temporal properties of MUA change as a function of the mouse response delays.

Next, we investigated whether the temporal properties of MUA, and more specifically those of responses evoked by the trained whiskers, covaried with the mouse behavior. We took advantage from the fact that, after training, the performance of mice in terms of timing was highly variable.

Fig. 3A1 shows for all mice the mean whisker-evoked MUA recorded in the layer 4 of the B column in response to stimulation of the B (PW), A (SW), and C (trained SW) whiskers. Sorting the MUA response according to the mouse NPD (first 5 trials) revealed striking correlations between mean spike delay (msd; see method) and mouse behavioral delay, and this relationship was strongest when the trained whisker was deflected (Spearman, r = 0.9; $p = 0.06 \times 10^{-5}$; n = 17; Fig. 3A). Whether mice exhibited whisker-triggered defensiveness or not during training did not impact the correlations (Fig. 3A2, compare symbols with red and black contours). Although still significant, the correlation decreased when NPD was sampled from the entire training session (r = 0.6; $p = 0.01$), suggesting motivation was one contributing factor. The firing rate in the population response to the trained whisker did not correlate with the NPD (r = -0.1; $p = 0.6$, Fig. 3B) and the MUA msd decreased compared to that of naive mice (-3.6 ms; Fig. 3A1; Mann-Whitney, $p = 0.06$), strengthening the hypothesis of temporal coding. The differences of MUA msd across trained animals could be caused by responses of variable lengths or variable onsets. The duration of the responses to the trained whisker did not co-vary with the mouse NPD (r = 0.1; $p = 0.7$) whereas the onset did (r = 0.8; $p = 0.0004$), showing that the whole response moved away from the stimulation onset in slower animals. We observed a different pattern of correlation for the response to the PW B: the interruption not the onset of this response co-varied with the mouse NPD (r = 0.5; $p = 0.03$). This finding is consistent with our earlier observation that it is principally the tail of responses to PW that is changed in trained mice. Strikingly no correlation was observed between NPD and the timing of neuronal responses evoked in the column corresponding to the trained whisker (Fig. 3C). Thus, changes in the timing of neuronal responses predicted the delay of the mouse behavioral response in the secondary column (B) but not in the primary column (C). This result was strengthened by the fact that the timing of the neuronal responses recorded in the tertiary column (A) were also correlated with the NPD (r = 0.8; $p =$

0.01; n = 9; Fig. 3D) despite that the stimulated whisker was 2 rows away from the principal whisker A.

The correlations between neuronal delays and mouse NPD were investigated for the layers 2/3 and 5A (Fig. 4A). The matrices indexing the Spearman correlation factor rho computed for every combination of whiskers (vertical axis in Fig. 4B) and cortical columns (horizontal axis) showed a similar pattern for the timing of responses evoked in the layer 5A. No correlation was found in layer 2/3. This was not because responses in layer 2/3 were too weak because those included in this analysis had similar firing rates than in layer 4 (mean C-evoked response = 6.4 ± 1.5 spikes in layer 2/3 and 7.6 ± 1.2 spikes in layer 4 of the B column).

Mice were stimulated with different durations over the length of a training session (see Methods). Thus, whisker stimulation *alone* could be responsible for the fact that L4 and L5A MUA in the B and A columns have different delays across mice. Several lines of evidence argue against this hypothesis. First, MUA msd was better correlated to the NPD sampled from the first five trials than to the total amount of stimulation mice received during the last training session. Correlation with total duration was still relatively high for C-evoked MUA in the layer 4 of the B column (r = 0.8; p = 0.001; n = 17) but absent in layer 5A (r = 0.6; p = 0.1; n = 10). Second, change in MUA timing was not associated to a change in MUA size (B column, L4, C whisker stim.; r = -0.002; p = 0.9; msd versus firing rate) which was expected if whisker stimulation per se drove the plasticity of neuronal responses here (Benedetti et al. 2009; Engineer et al. 2004; Wallace and Fox 1999). Finally, MUA timing and number of rewards did not correlate (B column, L4; r = -0.3; p = 0.3). Overall, these results make unlikely the hypothesis that neuronal delay in naive columns is a consequence of whisker stimulation or of positive reinforcement alone. Rather it suggests a link with the animal motor response.

Layer 4 and layer 5A receive inputs from thalamic nuclei of two distinct sensory integration pathways: L4, lemniscal; L5A, paralemniscal (Ahissar et al. 2000; Bureau et al. 2006; Koralek et al. 1988). To investigate whether a differential modulation of these pathways was contingent of the modulations of timing, we analyzed the size of layer 4 and layer 5A MUA across mice. In the B column, responses to the trained whisker with short latencies were associated to neuronal activation stronger in layer 5A than in layer 4 (Fig. 4C). The L4-L5A MUA size differential and the msd of L4 MUA correlated in this column ($r = 0.8$; $p = 0.01$; $n = 9$). There was no correlation in the column of the trained whisker ($r = 0.04$; $p = 0.9$; $n = 10$). To summarize, after associative learning, the neuronal population responses recorded in layer 4 and 5A, one and two columns away of the column of the trained whisker, are changed in ways that correlate with how fast animals accomplish the task.

Ex vivo, the layer 4 to layer 2/3 projection is weaker

The timing of layer 2/3 responses to stimulations of the trained whisker did not display any obvious relationship with the NPD, despite clear changes observed in layer 4. Because of the strong connectivity between these two layers, one might have expected responses in layer 2/3 to follow those of layer 4. This apparent inconsistency could be resolved if training changed the way spiking activity in layer 2/3 was controlled by layer 4. To test this hypothesis we used an in vitro approach in which glutamate uncaging at multiple sites across the cortical layers was combined with the recording of synaptically-evoked LFP in layer 2/3 (Fig. 5A,B). Amplitudes of synaptic events were reported in two dimensional matrices, also referred to as input maps. The section plane allowed identifying the A-E barrels and columns in the slice (Methods; Finnerty et al. 1999). Inputs maps of naive mice exhibited the typical organization of cortical circuits with a strong ascending projection from the layer 4 neurons to layer 2/3 neurons (Fig. 5C; Erlandson et

al. 2015). However, our recordings post training demonstrate associative learning induced a strong depression of this projection in the B and C columns (~ -50 %; $p < 0.05$; Fig. 5C). Noticeably, in the column of the trained whisker C, the depression was correlated with NPD sampled from the first five trials (r = 0.7; $p = 0.01$; n = 12; Fig. 5D,E). It was not correlated with the total amount of time mice were stimulated in the last session (r = 0.1; $p = 0.8$), suggesting here again a link with the mouse motor response rather than with stimulus. Inhibitory synaptic currents have little impact on the size of evoked LFP in this experimental setting (Erlandson et al. 2015). Thus, this training-induced depression can directly be interpreted as a weakening of the layer 4 to 2/3 excitatory projections. Underlying mechanism could be a decrease in synaptic strength, in the connectivity rate and/or in layer 4 neuron excitation. The decrease of layer 2/3 MUA is milder in vivo (- 20 %, Fig. 2E) (Gdalyahu et al. 2012). This suggests that after training neurons in layer 2/3 of barrel cortex are driven by new inputs. Those could be from the secondary somatosensory cortex (Kwon et al. 2016) but also from local horizontal projections (Rosselet et al. 2011). The latter could not be investigated here because their contribution to the input maps computed from local field potentials are underestimated (Erlandson et al. 2015).

Discussion

In this study, we designed a novel task in which mice freely moving in an arena can estimate the probability of a reward based on the presence or absence of a prolonged stimulation of their whisker. We found that, following training, mice effectively used this sensory cue to initiate runs toward the reward delivery location. Noticeably mice exhibited a wide range of delays in their behavioral response following whisker stimulation. We then performed in vivo

electrophysiological recordings of the spiking activity of neuronal populations in the barrel cortex of the trained mice. We report a strong correlation between the delay of population response to stimulation of the trained whiskers and the behavioral delay observed during task performance. Interestingly this correlation was found in recordings performed outside the principal column of the trained whisker. Our data reveal a new form of plasticity operating in barrel cortex that predicts how fast animals accomplish the task commanded by whisker stimulation.

Recently, a link was established between decision and the fine temporal distribution of spikes in responses evoked in barrel cortex during a sensory discrimination task (Zuo et al. 2015). In addition to the nature of decision taken, how fast actions are executed in response to the presentation of the sensory cues is a critical parameter of the behavioral responses. This delay in behavioral response is assumed to be constrained by the difficulty of the sensory discrimination task (e.g., the ambiguity of the stimuli) and by internal factors such as the cost associated with erroneous responses or the motivation of the animals (this study; Reinagel 2013; Bermudez and Schultz 2014; Berditchevskaia et al. 2016). Here we observed that mouse responses in a task with whisker deflections could also be delayed by sensory-triggered defensiveness (He et al. 2017). The neural mechanisms constraining behavioral delays have been intensively investigated in the visual-occulomotor system of monkeys. Neuronal correlates of reaction times in simple or delayed go/no-go tasks were found in the motor thalamus, the frontal eye field and the lateral intraparietal cortex (Hanes and Schall 1996; Roitman and Shadlen 2002; Janssen and Shadlen 2005; Tanaka 2007). In these studies ramping spiking activities were observed during the behavioral delays, which suggested that the timing of action performance was constrained by an accumulation of information that eventually crossed a decision boundary (Mazurek et al. 2003). Ramps of spiking activity have also been reported in the anterior lateral motor cortex in mice

accomplishing a delayed go/no-go task that involved whiskers suggesting that similar accumulative processes may contribute to the timing of decision making in tasks with tactile stimuli (Li et al. 2016). Here we provide evidence for a new form of neural correlate of behavioral delay in the barrel cortex. We found that the latency of neuronal discharges in response to whisker stimulation in the secondary columns of the trained whiskers predicted if mice were quick or slow to accomplish the task. It must be noted that the timescales of neuronal and behavioral delays measured in our study are quite different (respectively tens of milliseconds and seconds). It appeared that mice decided when to run based on the integration of multiple and at times conflicting information linked to sensory perception and to motivation. It is then remarkable that the correlation between neuronal delay and behavioral delay was strong despite the multiplicity of causes underlying the latter. The observation that the correlation is stronger when the first trials only are taken into account suggests a powerful effect of the whisker/reward association onto neuronal circuits early on during the session, before satiety grows. This modulation of neuronal delays concurred with the differential modulation observed in vivo of layer 4 and layer 5A activation in the secondary column, which could indicate changes in the balance of the lemniscal drive and paralemniscal drive. The activation of the layer 5A dominated in mice with fast neuronal responses. Another contingency was the depression of the major projection from the layer 4 to the superficial layers. Overall these observations suggest that associative learning together with the integration of internal factors tune the relative activation of layer 4 and layer 5A evoked by the trained whisker and regulate the timing of neuronal responses in naive cortical columns as well as they are shaping the mouse behavioral response to whisker stimuli.

The correlation between NPD and neuronal delays in the B column was strongest when the C (trained) whisker was stimulated and gradually decreased for the B and A whisker stimulation. It is unlikely that this effect is caused by a collateral stimulation of A and B whisker during the task, as we verified that our electromagnetic stimulation of the C whiskers did not induced noticeable deflections of neighboring whiskers. Moreover when recordings were performed in the C column there was no correlation between NPD and neuronal delays in responses to the B and A whiskers, which would be expected if these whiskers had also been stimulated in the conditioning arena. Interestingly, we reported that mice quickly transferred the association between C whisker stimulation and reward delivery to the stimulation of adjacent whiskers. This finding is reminiscent of the observation made by Diamond and collaborators (Diamond et al. 1999) that rats quickly reacquire their performance at crossing a gap if the whisker used in the task moves of one row. A parsimonious explanation for both the fast transfer of learning to neighboring whiskers and the graded correlations between NPD and neuronal delays in responses to A, B and C whisker stimulation is that the circuits integrating the C whisker inputs partially overlap with the circuits of A and B whiskers in barrel cortex (Diamond et al. 1999).

The finding that neuronal delays in cortical columns of non-trained whiskers predict the timing of animal behavior is in agreement with previous studies reporting that neuronal activity predictive of a decision is found in several cortical columns (Yang et al. 2016). It is also consistent with the observation that the neuronal activity in barrel cortex involved in decision making is, in the chain of events triggered by the deflections of whiskers, downstream of the primary feedforward thalamic drive (Sachidhanandam et al. 2013; Yang et al. 2016). Still, it is intriguing that no correlations between MUA response delay and mouse NPD were observed in the cortical column of the trained whisker as previous studies reported that activity in this column predicted the

occurrence of sensory-guided behavioral responses (Yang et al. 2016). First, this could indicate that the temporal properties of responses evoked in the column of the trained whisker are changed in a more uniform manner across mice, precluding a correlation with the mouse NPD. Second, this could indicate that associative learning has a differential impact on properties of responses evoked by PW and SW (Fig. 2D). This is supported by the differences we found between the neuronal responses recorded in the B column following stimulations of the C (secondary) whisker and B (principal) whisker. When the C whisker was stimulated, the delay of the neuronal response increased according to the NPD but the response duration was unchanged across animals. When the PW was deflected, the end not the onset of responses changed in a correlated manner with the NPD. This suggests that a consequence of associative learning for responses to PWs is to change the delay of a late component. A late-onset component of a PW-evoked response drove behavioral decision in the study of Sachidhanandam and collaborators (Sachidhanandam et al. 2013). Here, early and late components may be intermingled in the column of the trained whisker, enough to confound the correlation between the PW-evoked response delay and mouse NPD.

Our findings point to differences across trained mice in the delay of activation of cortical columns upon whisker stimulation. How can such differences emerge? A first possibility is that responses are shaped by the interplay between local excitatory and inhibitory circuits allowing the fine modulation of speed with which inputs are propagated horizontally in cortex (Sachidhanandam et al. 2015; Petersen and Sakmann 2001) (Fig. 6). We previously showed that pairing the deflections of the C whiskers with tail shocks created novel excitatory projections from the layer 4 of the C column to the B column (Rosselet et al. 2011). This finding contrasts with the canonical description of networks of sensory cortex which organizes intracortical

connections into columnar functional units. Our observations here that neurons in layer 2/3 are partially disconnected from their classical synaptic driver in layer 4 (Fig. 5) while showing little reduction in activity suggest also a profound remodeling of the functional wiring in the barrel cortex of trained mice. The increased correlation of spikes between the C and B columns in trained mice (Fig. 2I) would be consistent with a facilitated propagation of neuronal information in the horizontal axis. Alternatively, the responses evoked by the trained whisker in naive cortical columns could also originate from structures that have reciprocal innervations with barrel cortex: the thalamus, the secondary somatosensory cortex, the primary motor cortex or the perirhinal cortex (Aronoff et al. 2010). It was recently shown that the activity of axons from the secondary somatosensory cortex innervating the barrel cortex encoded perceptual decision in a detection task (Yang et al. 2016). These axons, dense in layer 1, could drive the activity of pyramidal cells with somata in layer 2/3 and layer 5. Yet, it is interesting that we did not find temporal coding in the layer 2/3 but only in thalamo-recipient layers, the layers 4 and 5A. The differential modulation of layer 4 and layer 5A activation suggests also the implication of thalamic inputs (Fig.6). In layer 4, the integration window of inputs sent by the ventral postero-medial nucleus (VPM) of thalamus could be controlled by feed-forward inhibition (Gabernet et al. 2005). The study of the neuronal activity in the posterior medial nucleus (POm) will be also of interest because of the loose somatotopic organization of its projections in the layer 5A (Deschenes et al. 1998; Bureau et al. 2006). The anatomical study of these projections could also unveil anisotropy in the way they innervate the barrel cortex to explain why temporal correlations were found in the B column but not in D when the C whisker was stimulated.

In conclusion, our study supports the role of the primary sensory cortex into the making of perceptual decision in rodents and points to new directions for investigating the mechanisms shaping the functional wiring in sensory areas of cortex.

Acknowledgements

The authors thank Dr Jérôme Epsztein of INMED and Dr Miguel Maravall of University of Sussex for critically reading earlier versions of the paper; and the staff of the animal facility at INMED for the daily care of animals. This work was supported by the Agence Nationale de la Recherche (grant number ANR-11-BSV4-0013) and the Human Frontier Science Program (grant number CDA - 0041 / 2007-C). MAE's thesis was supported by the Excellence Initiative of Aix-Marseille University - A*MIDEX (ICN PhD program). Current affiliation of J. Camon is UPRES EA 2647 | USC INRA 1330, University of Angers (Angers, France). Current affiliation of S. Hugues is E-Phy-Science, Sophia antipolis (Valbonne, France). Current affiliation of S. Lagoun is Center for brain research at Medical university of Vienna (Vienna, Austria). Address of corresponding author: ingrid.bureau@inserm.fr

References

Ahissar E, Sosnik R, Haidarliu S. 2000. Transformation from temporal to rate coding in a somatosensory thalamocortical pathway. Nature. 406:302-306.

Ahissar E, Sosnik R, Bagdasarian K, Haidarliu S. 2001. Temporal frequency of whisker movement. II. Laminar organization of cortical representations. J Neurophysiol. 86:354-367.

Aronoff R, Matyas F, Mateo C, Ciron C, Schneider B, Petersen CC. 2010. Long-range connectivity of mouse primary somatosensory barrel cortex. Eur J Neurosci. 31:2221-2233.

Benedetti BL, Glazewski S, Barth AL. 2009. Reliable and Precise Neuronal Firing during Sensory Plasticity in Superficial Layers of Primary Somatosensory Cortex. J Neurosci. 29: 11817-11827.

Berger D, Warren D, Normann R, Arieli A, Grün S. 2007. Spatially organized spike correlation in cat visual cortex. Neurocomputing. 70: 2112-2116.

Bermudez MA, Schultz W. 2014. Timing in reward and decision processes. Philos Trans R Soc Lond B. 369:20120468.

Bureau I, von Saint Paul F, Svoboda K. 2006. Interdigitated Paralemniscal and Lemniscal Pathways in the Mouse Barrel Cortex. PLoS Biol. 4:e382.

Cisek P, Kalaska JF. 2005. Neural correlates of reaching decisions in dorsal premotor cortex: specification of multiple direction choices and final selection of action. Neuron. 45:801-814.

Cisek P, Kalaska JF. 2010. Neural mechanisms for interacting with a world full of action choices. Annu Rev Neurosci. 33:269-298.

Deschenes M, Veinante P, Zhang ZW. 1998. The organization of corticothalamic projections: reciprocity versus parity. Brain Res Rev. 28:286-308.

Diamond ME, Petersen RS, Harris JA. 1999. Learning through maps: functional significance of topographic organization in primary sensory cortex. J Neurobiol. 41:64-68.

Engineer ND, Percaccio CR, Pandya PK, Moucha R, Rathbun DL, Kilgard MP. 2004. Environmental enrichment improves response strength, threshold, selectivity, and latency of auditory cortex neurons. J Neurophysiol. 92: 73-82.

Erlandson MA, Manzoni OJ, Bureau I. 2015. The Functional Organization of Neocortical Networks Investigated in Slices with Local Field Recordings and Laser Scanning Photostimulation. Plos One. 10:e0132008.

Finnerty GT, Roberts LSE, Connors BW. 1999. Sensory experience modifies the short-term dynamics of neocortical synapses. Nature. 400: 367-371.

Gabernet L, Jadhav SP, Feldman DE, Carandini M, Scanziani M. 2005. Somatosensory integration controlled by dynamic thalamocortical feed-forward inhibition. Neuron. 48: 315-327.

Gdalyahu A, Tring E, Polack PO, Gruver R, Golshani P, Fanselow MS, Silva AJ, Trachtenberg JT. 2012. Associative fear learning enhances sparse network coding in primary sensory cortex. Neuron. 75:121-132.

Gold JI, Shadlen MN. 2007. The neural basis of decision making. Annu Rev Neurosci. 30:535-574.

He CX, Cantu DA, Mantri SS, Zeiger WA, Goel A, Portera-Cailliau C. 2017. Tactile Defensiveness and Impaired Adaptation of Neuronal Activity in the Fmr1 Knock-Out Mouse Model of Autism. J Neurosci. 37:6475-6487.

Koralek KA, Jensen KF, Killackey HP. 1988. Evidence for two complementary patterns of thalamic input to the rat somatosensory cortex. Brain Res. 463:346-351.

Kwon SE, Yang H, Minamisawa G, O'Connor DH. 2016. Sensory and decision-related activity propagate in a cortical feedback loop during touch perception. Nat Neurosci. 19:1243-1249.

Li N, Daie K, Svoboda K, Druckmann S. 2016. Robust neuronal dynamics in premotor cortex during motor planning. Nature. 532:459-464.

Mazurek ME, Roitman JD, Ditterich J, Shadlen MN. 2003. A role for neural integrators in perceptual decision making. Cereb Cortex. 13:1257-1269.

Petersen CC, Sakmann B. 2001. Functionally independent columns of rat somatosensory barrel cortex revealed with voltage-sensitive dye imaging. J Neurosci. 21: 8435-8446.

Reinagel P. 2013. Speed and accuracy of visual image discrimination by rats. Front Neural Circuits. 7:200.

Rosselet C, Fieschi M, Hugues S, Bureau I. 2011. Associative learning changes the organization of functional excitatory circuits targeting the supragranular layers of mouse barrel cortex. Front Neural Circuits. 4:126.

Sachidhanandam S, Sreenivasan V, Kyriakatos A, Kremer Y, Petersen CC. 2013. Membrane potential correlates of sensory perception in mouse barrel cortex. Nat Neurosci. 16:1671-1677.

Sachidhanandam S, Sermet BS, Petersen CC. 2015. Parvalbumin-Expressing GABAergic Neurons in Mouse Barrel Cortex Contribute to Gating a Goal-Directed Sensorimotor Transformation. Cell Rep. 15:700-706

Shepherd GMG, Svoboda K. 2005. Laminar and columnar organization of ascending excitatory projections to layer 2/3 pyramidal neurons in rat barrel cortex. J Neurosci. 25:5670-5679.

Shepherd GMG, Pologruto TA, Svoboda K. 2003. Circuit analysis of experience-dependent plasticity in the developing rat barrel cortex. Neuron. 38:277-289.

Smith MA, Kohn A. 2008. Spatial and temporal scales of neuronal correlation in primary visual cortex. J Neurosci. 28: 12591-12603.

Suter BA, O'Connor T, Iyer V, Petreanu LT, Hooks BM, Kiritani T, Svoboda K, Shepherd GMG. 2010. Ephus: multipurpose data acquisition software for neuroscience experiments. Front Neural Circuits. 4:100.

Wallace H, Fox K. 1999. The effect of vibrissa deprivation pattern on the form of plasticity induced in rat barrel cortex. Somatosens Mot Res. 16: 122-138.

Yang H, Kwon SE, Severson KS, O'Connor DH. 2016. Origins of choice-related activity in mouse somatosensory cortex. Nat Neurosci. 19:127-134.

Zuo Y, Safaai H, Notaro G, Mazzoni A, Panzeri S, Diamond ME. 2015. Complementary contributions of spike timing and spike rate to perceptual decisions in rat S1 and S2 cortex. Curr Biol. 25:357-363.

Table 1. Properties of MUA evoked at three depths.

MUA of naive mice (n = 20)			
Depth	2 – layer 2/3 n_e = 49	3 – layer 4 n_e = 49	4 – layer 5A n_e = 47
Peak firing rate, SW, 1st stimulation (Hz)	160 ± 14 *0.0005*	261 ± 21	309 ± 21
TW/PW	0.17 ± 0.02	0.23 ± 0.03	0.31 ± 0.04
MUA of trained mice (n = 38)			
depth	2 – layer 2/3 n_e = 78	3 – layer 4 n_e = 92	4 – layer 5A n_e = 73
Peak firing rate, SW, 1st stimulation (Hz)	226 ± 18 0.0000001	361 ± 18	350 ± 22
TW/PW	0.25 ± 0.03 0.05	0.35 ± 0.03	0.47 ± 0.04 0.03

Values are mean ± SEM and *p*. They are from recordings in the B, C and D columns, combined. In italic, the *p* values indicate significant differences with layer 4. n_e is the number of electrodes. Same data as in Fig.2.

Figure 1: Operant conditioning task guided by the magnetic stimulation of whiskers.

A, Schematic of a session. In go trials, the whiskers C1 and C2 on which a metal rod was glued are deflected and the mouse has ten seconds to approach the water port to be rewarded. The reward is unavailable for the first three seconds (delay period). Then, the water port is operational for seven seconds. Parameters measured are the NPD, or the delay prior a first nose poke is made in the water port, and the length of visits initiated during the three second delay period; **B**, Left, two snapshots of the arena showing a mouse going to the water port (black rectangle at the top). Right, schematic of the arena showing the trajectories made by a mouse in three go trials. The color codes for the elapsed time since the stimulation onset. The water port is in black. The white semi-circle delineates the "stimulation area" where mice had to enter in order for the whisker stimulation to start in go trials. Note that this area is invisible to mice as the entire platform is white. **C**, The presence of the black mouse at the water port was detected thanks to contrast with the white platform. Gray levels measured at the water spout as a function of time for three go trials (top, same as in B) and three catch trials (bottom). The orange arrows indicate the first nose poke (NP) at the water port made at each trial; The blue shaded areas, the periods during which a reward was delivered. **D**, Removing the whisker stimulation increased the NPD and dissipated the difference between go and catch trials (n = 3). NPD were sampled from the entire session, with and without cue. **E**, Moving the stimulation from the C whiskers (black) to the B whiskers (red) had a labile effect on NPD measured in go trials (n = 12). In gray, the NPD during the first training session. **F**, The time spent at the water port for visits that occurred during the delay period (i.e., for NPD < 3 s). Left, go trials; Right, catch trials. Each symbol is a mouse. The red dashed lines indicate the maximum length of visits for each NPD (e.g., 2 s for a NPD of 1 s, 1.5 s for a NPD of 1.5 s …). Note how symbols were closer to the dashed line in go trials indicating that mice stayed longer at the water port. **G**, Cumulative distribution of the ratio of time actually

spent (true) at the water port during the delay period over the maximum value it could have been (max). The red dashed line indicates 100 % (same data as in F). Black, go trials; Grey, catch trials. **H**, NPD for mice with (white, n = 34) and without (red, n = 18) whisker-triggered defensive behavior. The thick black line shows the median, the box the 25^{th} to 75^{th} percentiles and the whiskers the upper and lower bounds of the distribution. **I**, The NPD from catch trials as a function of NPD from go trials. Red line, the NPDs correlated for mice without whisker-triggered defensive behavior (red symbols; r = 0.5; $p = 0.04$).

Figure 2: Training affected mostly the multi-unit activity evoked by non-principal whiskers. **A**, Schematic of the vivo electrophysiological recordings. A to D whiskers of arc 1 or arc 2 were stimulated individually with glass capillaries glued on benders (A1). Only two of four capillaries are shown. An 8-shank-by-4 site silicon probe was lowered in arc 1 or arc 2 (blue) of barrel cortex. MUA were recorded at four depths in multiple columns (spacing, 200 μm; A2). Sites selected for further analysis (blue) were on shanks where the A, B, C or D whisker had evoked its largest response. The shanks were hereafter referred as functional cortical columns and were each assigned one functional principal whisker. **B**, Averaged MUA from a naive mouse recorded in the C column. The stimulation was a train of three deflections of the principal whisker (PW) C (black), or from the secondary whiskers (SW) B (orange) and D (green). **C**, Properties of MUA allowed resolving three layers, 2/3-4-5A, in naive mice (C1) and in trained mice (C2). The short-term depression (STD) is the ratio of peak amplitude of responses evoked at the fifth pulse and first pulse of the stimulation train. SW/PW is the ratio of peak amplitude of responses evoked by SW and PW. Sample sizes are in table 1 (same data). **D**, training affected the temporal course of MUA evoked by SW principally. Traces are the median MUA evoked in the layer 4 of the C and

B cortical columns. **E**, Same data as in D but responses are aligned on their center of mass. Amplitudes are normalized to the max. Shaded areas contain values between the 25^{th} and 75^{th} percentiles. **F**, Temporal accumulation of spikes in layer 2/3-4-5A MUA evoked by SW. Arrow heads indicate MUA center of mass. Responses to SW were more compact in trained mice. The thick lines are the median values, the shaded areas the values between the 25^{th} and 75^{th} percentiles. Data are from recordings in the B and C columns when the B or C whisker was stimulated. **G**, Spike count (left) and coefficient of variation of spike count (right) integrated within 100 ms of the stimulus onset for the three layers. * is $p < 0.05$. **H**, Example of a cross-correlogram (CCG) of MUA evoked by the stimulation of the C whisker and recorded in the layer 5A of the B and C columns. Raw CCG (gray bars) was computed on the time resolution of 1 ms (the trace is smoothed). Original data were resampled to compute a correction term (thick line). The dotted line is the significance level (correction term plus twice the standard deviation). In blue, the corrected CCG is the raw CCG above significance level minus the correction term. **I**, Probability per spike (at the peak). Number of CCG for naive and trained mice is 22 and 16 (layer 2/3), 20 and 30 (layer 4), 22 and 16 (layer 5A). * is $p < 0.05$. Data are from recordings in the B and C columns when the B or C whisker was stimulated.

Figure 3: The responses evoked by the trained whisker shifted temporally as a function of the delay of the mouse behavioral response.

A, averaged MUA stacked as a function of the delay prior the first nose poke at the water port (NPD). Each line is the MUA from a mouse normalized to its maximum firing rate. Top (A1), MUA evoked by the A to C whiskers and recorded in the layer 4 of the B column. C* is for the trained C whisker. Open magenta symbols are the mean spike delay (msd) of MUA evoked by the trained whisker C. Note how the msd of MUA increased for mice with longer NPD. Box-and-

whisker plots are the MUA msd of C-evoked MUA in the B column of trained mice (light magenta, n = 17) and naive mice (gray, n= 12). Each box shows the lower quartile, median (vertical white line), and upper quartile values. Whiskers show the minimum and maximum of the distribution. Mann-Whitney test, p = 0.06. Bottom (A2), Plots showing the MUA msd as a function of the mouse NPD. Symbols with red contours are for mice without whisker-triggered defensiveness. r is the Spearman correlation factor rho. **B**, Top (B1), responses to C evoked in the layer 4 of the B column (same as in panel A1) with a different color scale to show the firing rates. Bottom (B2), firing rate and NPD did not correlate. **C,** Top (C1), MUA evoked by the B and C whiskers and recorded in the layer 4 of the C column. Open magenta symbols are the msd of MUA evoked by the trained whisker C. Bottom (C2), the MUA msd as a function of the mouse NPD. **D**, Same as in C for the responses to the trained whisker C evoked in the layer 4 of the A column.

Figure 4: Modulation of neuronal delays was associated to a differential modulation of layer 4 and layer 5A activation.

A, Left (A1), MUA evoked by the C whisker and recorded in the layer 5A and layer 2/3 of the B column stacked as a function of NPD. See Fig. 3A for details. Right, (A2), the MUA msd as a function of the mouse NPD. They correlated in layer 5A but not in layer 2/3. Symbols with red contour are for mice without whisker-triggered defensiveness. **B**, Top, matrices indexing the rho factor of the Spearman correlation between NPD and MUA msd computed for every combination of whiskers (horizontal axis) and cortical columns (vertical axis) for the three layers. Bottom, matrices indexing the statistical significance of each correlation (p). Numbers of electrodes are 9 17 23 14 in the layer 4 of A B C D column, respectively. They are 5 10 12 9 in layer 5A (ABCD) and 11 11 7 in layer 2/3 (BCD). **C**, Relative activations of layer 4 and layer 5A evoked by the

stimulation of the trained whisker C as a function of the msd of layer 4 MUA, for the B and C column. The Y axis displays the values computed from: $(F_{L4}- F_{L5})/ F_{L4}$ where F is the firing rate evoked within 50 ms of stimulation onset. r is the Spearman correlation factor rho.

Figure 5: Training weakened the ascending projections onto layer 2/3 neurons.

A, Schematic of the electrophysiological recordings in brain slices. Two pipettes were placed above the B and C barrels in layer 2/3 for recording local field potentials. The center of the uncaging grid (blue) for stimulating neurons was aligned horizontally with the barrel B and C boundary. The blue dots with numbers are the sites of glutamate uncaging that evoked the responses shown in B. **B**, Examples of local field potentials. They were either direct responses (traces 1 and 2) when glutamate was uncaged on the top of the soma or dendrites of recorded neurons. Then, they were either negative when evoked in the vicinity of the recording pipette or positive when evoked further away. Local field potentials were synaptic when responses had a few ms latency (> 5 ms; trace 3). They were due to the activation of monosynaptic connections made between the neurons excited at the uncaging site and the recorded neurons. The blue and green shades indicate the time windows for separating direct and synaptic events. **C,** Averaged input maps for recordings made in the layer 2/3 of the B and C columns in the naive and trained mice. Data from the B and C columns are merged for the naive mice. The color of pixels codes for the peak amplitude of the evoked field postsynaptic potentials (fPSP) averaged across recordings. Circles are recording locations, the dashed lines mark the layer 4. The grey areas mask sites where glutamate uncaging evoked direct responses. **D**, Stack of input maps recorded in layer 2 and layer 3 of the B and C columns that were compressed horizontally so that each column of pixels corresponded to one recording. Mice were ordered according to their NPD. Between the arrows is the layer 4. The grey areas mask sites with direct responses. Input maps

from the C column showed that layer 4 to layer 2/3 projections were weaker in mice with fast behavioral responses. **E,** Strength of layer 4 inputs received by layer 2 and layer 3 neurons in the C column (two left panels) and B column (two right panels) as a function of the mouse NPD. Symbols with red contour are for mice without whisker-triggered defensiveness. Dashed lines are the averaged values obtained in naive mice.

Figure 6: Potential functional rewiring in barrel cortex following operant conditioning.

Left, naive animal. Right, after training. Black arrows, flows of inputs from the trained whisker C. Light gray arrows, the same for the B whisker. These inputs originate from the lemniscal nucleus (ventral postero-medial or VPM) in thalamus. Shown as dark gray arrows, the flows of inputs originating from the paralemniscal nucleus in thalamus (posterior medial or POm) go to layer 5A in the B and C columns. Arrows with chevron: after training, circuits within barrel cortex and/or originating from POm could disseminate inputs from the trained whisker C in the B column with a speed that is function of the animal behavioral timing in the task. Cortical responses could be shaped by the strength and dynamic of excitatory and inhibitory circuits and by intrinsic properties of neurons. Dotted arrows indicate flows of inputs that could be weaker in animals that accomplish the task quickly. Activity in layer 2/3 could be driven for a part by inputs from the secondary somatosensory cortex after training.

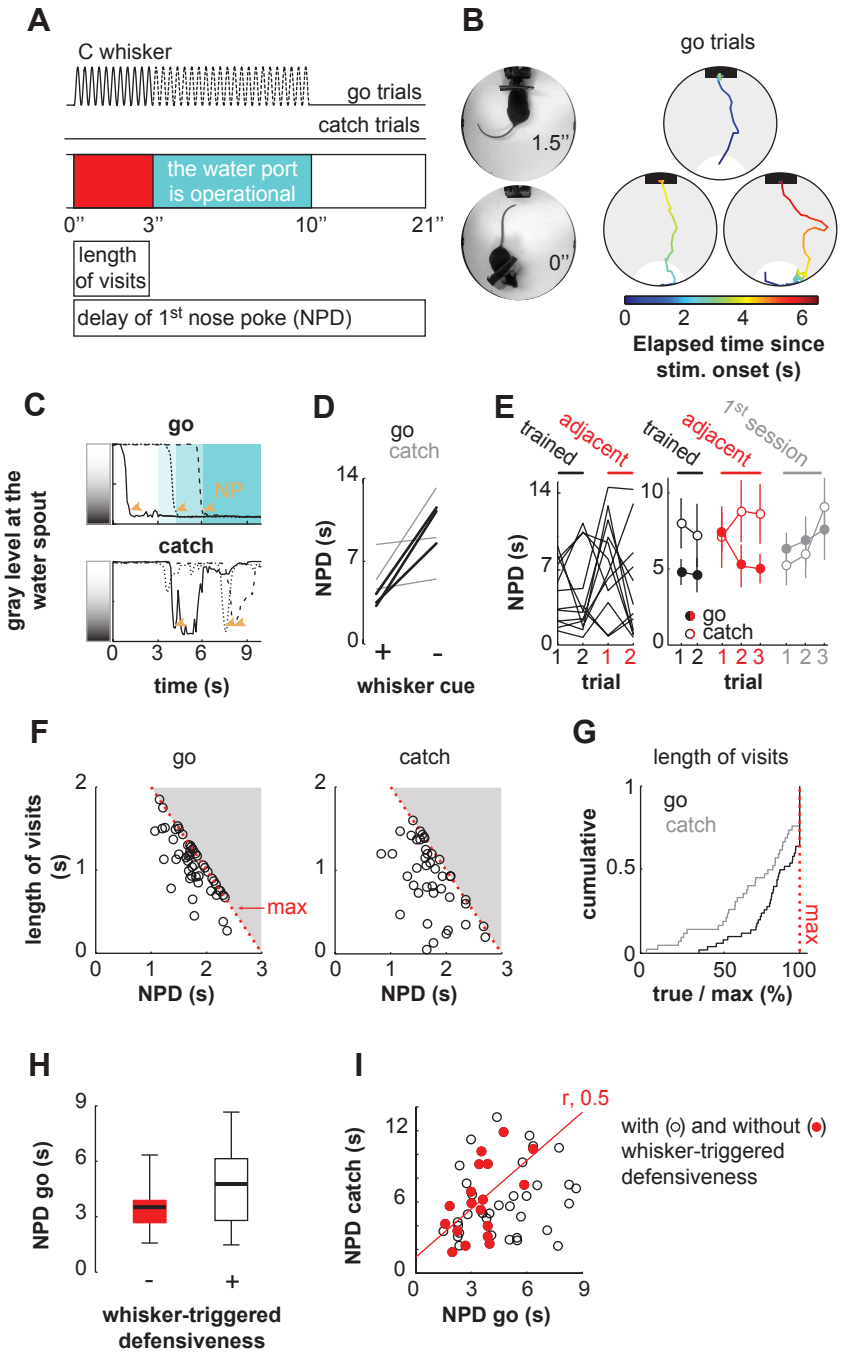
A
C whisker
go trials
catch trials
the water port is operational
0"
3"
10"
21"
length of visits
delay of 1st nose poke (NPD)
B
go trials
1.5"
0"
0
2
4
6
Elapsed time since stim. onset (s)
C
go
catch
NP
gray level at the water spout
0
3
6
9
time (s)
D
go
catch
NPD (s)
14
7
0
+
-
whisker cue
E
trained
adjacent
trained
adjacent
1st session
NPD (s)
trial
go
catch
F
go
catch
length of visits (s)
max
NPD (s)
G
length of visits
go
catch
cumulative
max
true / max (%)
H
NPD go (s)
whisker-triggered defensiveness
I
r, 0.5
NPD catch (s)
NPD go (s)
with (○) and without (●) whisker-triggered defensiveness

Figure 1

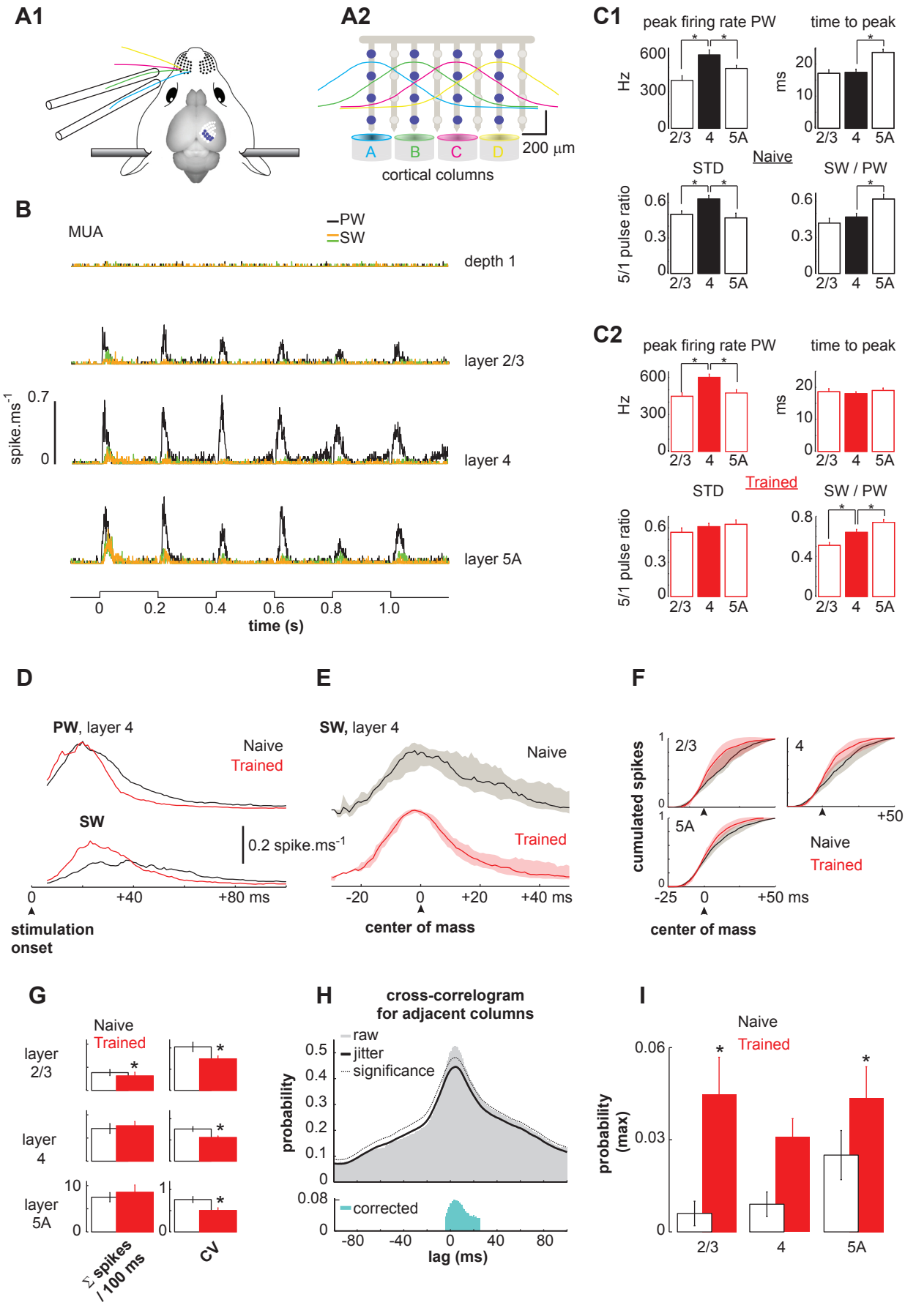
A1
A2
A
B
C
D
200 µm
cortical columns
B
MUA
PW
SW
depth 1
layer 2/3
layer 4
layer 5A
spike.ms-1
0.7
0
0
0.2
0.4
0.6
0.8
1.0
time (s)
C1
peak firing rate PW
time to peak
Hz
ms
600
300
0
20
10
0
2/3
4
5A
Naive
STD
SW / PW
5/1 pulse ratio
0.6
0.3
0
C2
Trained
0.8
0.4
D
PW, layer 4
Naive
Trained
SW
0.2 spike.ms-1
0
+40
+80 ms
stimulation onset
E
SW, layer 4
-20
+20
+40 ms
center of mass
F
cumulated spikes
1
2/3
4
5A
+50
-25
+50 ms
G
layer 2/3
layer 4
layer 5A
10
1
Σ spikes / 100 ms
CV
H
cross-correlogram for adjacent columns
raw
jitter
significance
probability
0.5
0.4
0.3
0.2
0.1
corrected
0.08
-80
-40
40
80
lag (ms)
I
probability (max)
0.06
0.03

Figure 2

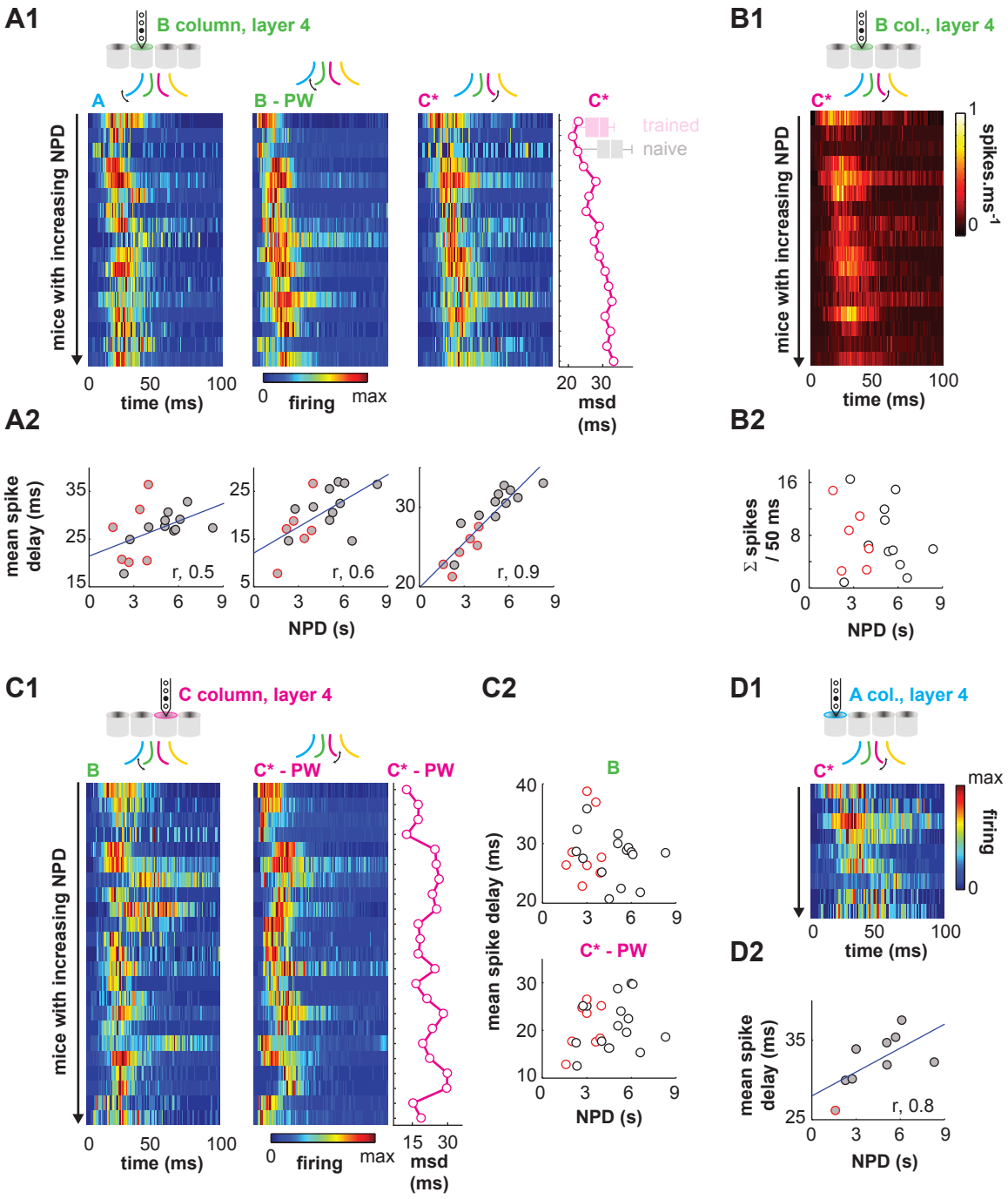
A1
B column, layer 4
A
B - PW
C*
C*
trained
naive
mice with increasing NPD
0
50
100
time (ms)
0
firing
max
20
30
msd
(ms)
B1
B col., layer 4
C*
1
spikes.ms-1
0
mice with increasing NPD
0
50
100
time (ms)
A2
mean spike delay (ms)
35
25
15
r, 0.5
25
15
5
r, 0.6
30
20
r, 0.9
0
3
6
9
NPD (s)
B2
Σ spikes / 50 ms
16
8
0
0
3
6
9
NPD (s)
C1
C column, layer 4
B
C* - PW
C* - PW
mice with increasing NPD
0
50
100
time (ms)
0
firing
max
15
30
msd
(ms)
C2
B
40
30
20
0
3
6
9
C* - PW
30
20
10
0
3
6
9
mean spike delay (ms)
NPD (s)
D1
A col., layer 4
C*
max
firing
0
0
50
100
time (ms)
D2
mean spike delay (ms)
35
25
r, 0.8
0
3
6
9
NPD (s)

Figure 3

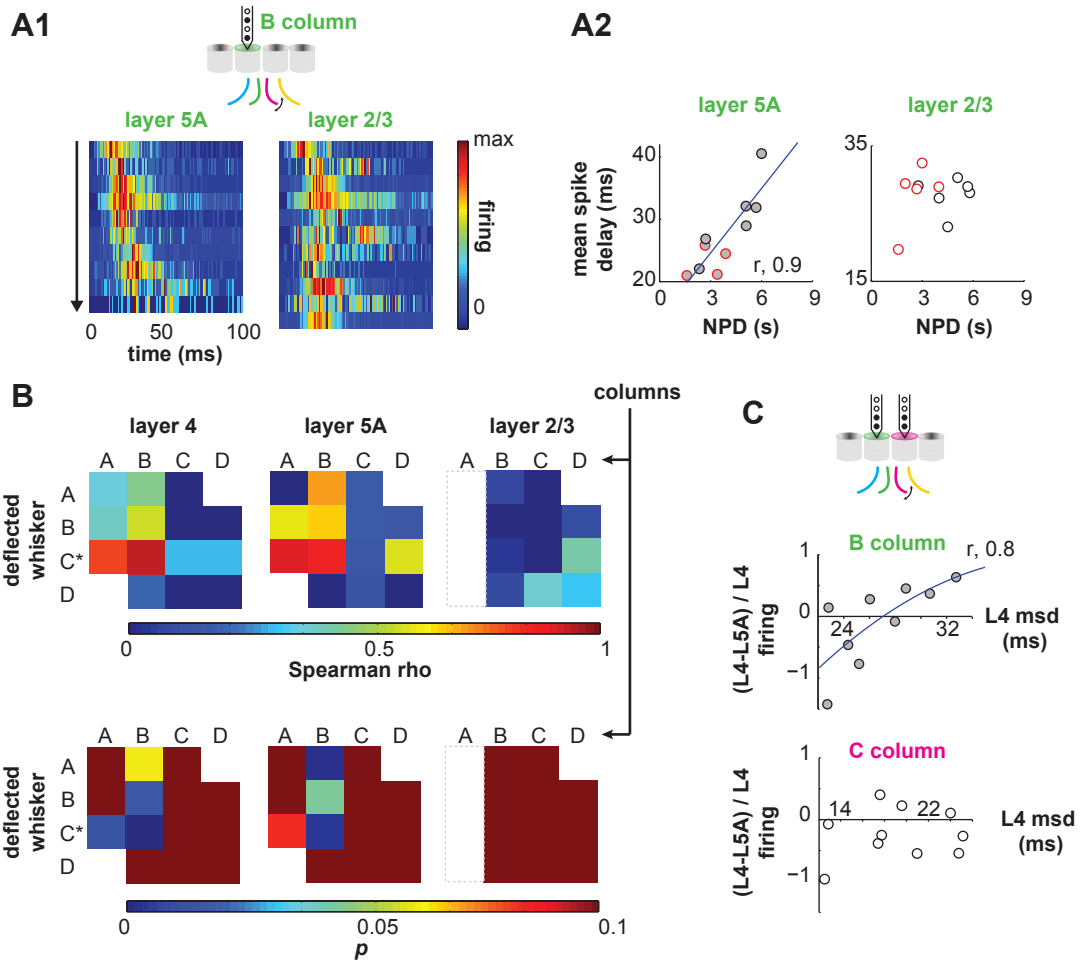
A1
B column
layer 5A
layer 2/3
max
firing
0
0
50
100
time (ms)
A2
layer 5A
layer 2/3
mean spike delay (ms)
40
30
20
r, 0.9
0
3
6
9
NPD (s)
35
15
0
3
6
9
NPD (s)
B
columns
layer 4
layer 5A
layer 2/3
A B C D
deflected whisker
A
B
C*
D
0
0.5
1
Spearman rho
p
0
0.05
0.1
C
B column
r, 0.8
(L4-L5A) / L4 firing
1
0
−1
24
32
L4 msd (ms)
C column
14
22
L4 msd (ms)

Figure 4

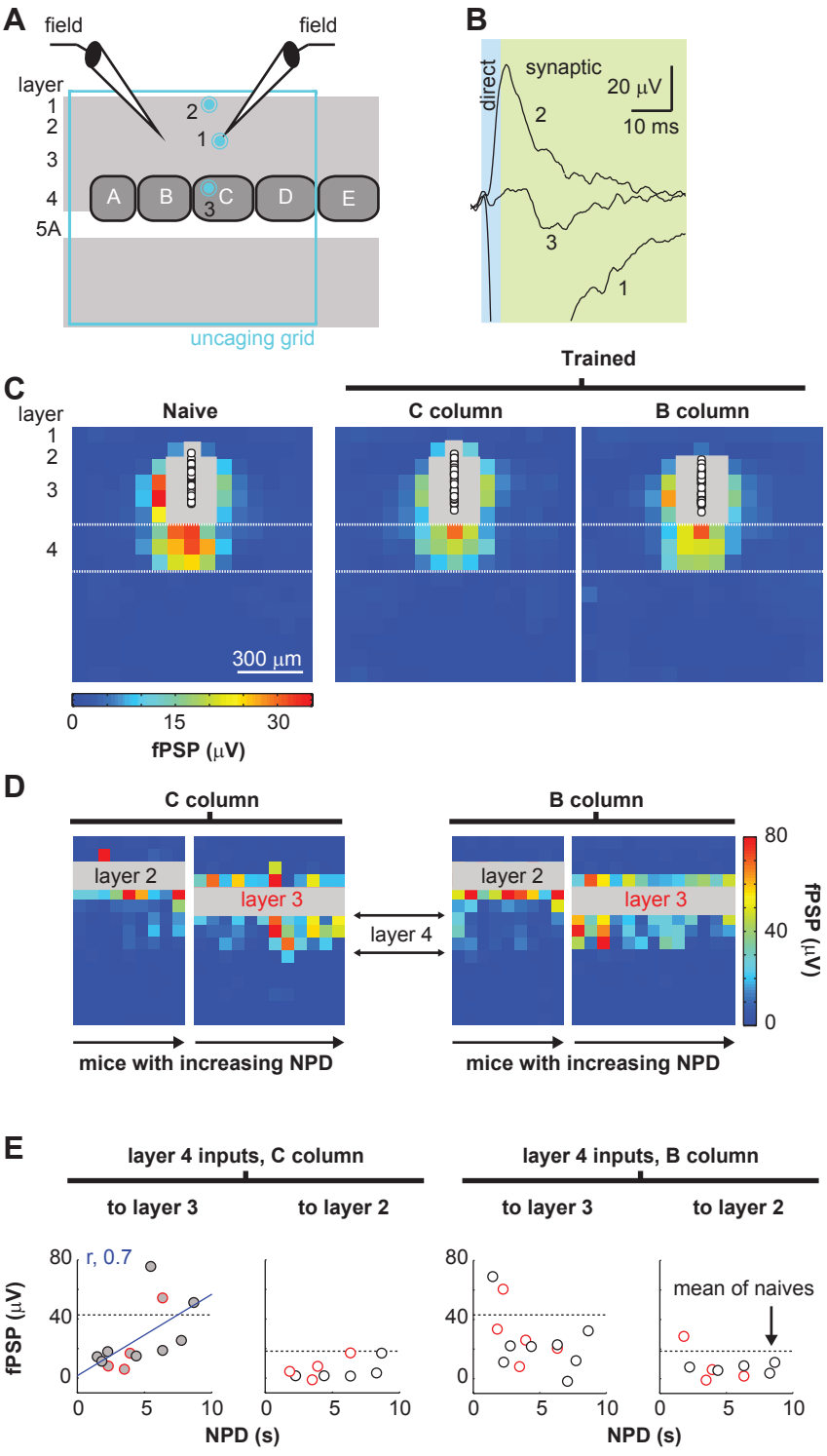
A
field
field
layer
1
2
3
4
5A
2
1
3
A
B
C
D
E
uncaging grid
B
direct
synaptic
20 μV
10 ms
2
3
1
C
Trained
layer
Naive
C column
B column
1
2
3
4
300 μm
0
15
30
fPSP (μV)
D
C column
B column
layer 2
layer 3
layer 4
layer 2
layer 3
80
40
0
fPSP (μV)
mice with increasing NPD
mice with increasing NPD
E
layer 4 inputs, C column
layer 4 inputs, B column
to layer 3
to layer 2
to layer 3
to layer 2
80
40
0
r, 0.7
fPSP (μV)
0
5
10
NPD (s)
mean of naives
NPD (s)

Figure 5

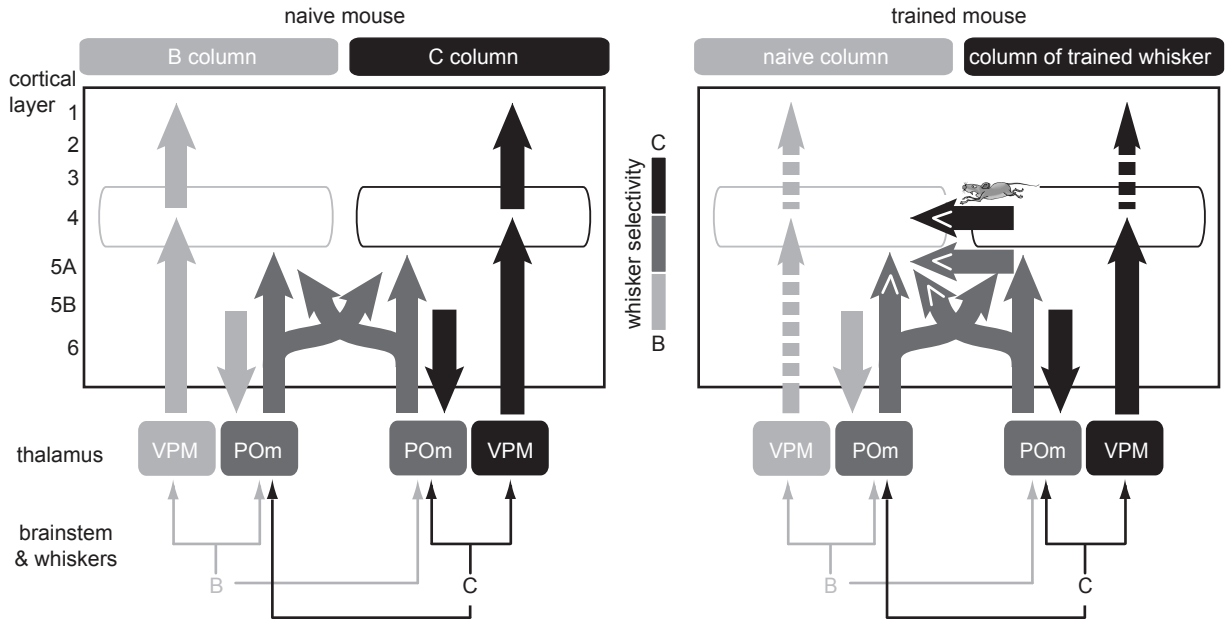
naive mouse
B column
C column
cortical layer
1
2
3
4
5A
5B
6
thalamus
VPM
POm
POm
VPM
brainstem & whiskers
B
C
whisker selectivity
C
B
trained mouse
naive column
column of trained whisker
VPM
POm
POm
VPM
B
C

Figure 6